International Conference on Mathematics, Computational Methods & Reactor Physics (M&C 2009)
Saratoga Springs, New York, May 3-7, 2009, on CD-ROM, American Nuclear Society, LaGrange Park, IL (2009)

ANALYSIS AND BENCHMARKING OF PENTRAN CODE USING THE OECD-NEA BENCHMARK PROBLEMS

Alireza Haghighat, Glenn E. Sjoden and Ce Yi
University of Florida
Department of Nuclear and Radiological Engineering
202 Nuclear Science Building, Gainesville, Florida, USA
haghighat@ufl.edu, sjoden@ufl.edu, yice@ufl.edu

ABSTRACT

It is our pleasure to be able to contribute this paper to a special session honoring Dr. Enrico Sartori, whose effort and devotion have resulted in significant international collaborations, enhancement in particle transport methods and various reactor physics problems through benchmarking, and ease of access to latest nuclear data and nuclear codes. In this paper, we overview our past efforts in benchmarking the PENTRAN code using different OECD-NEA benchmark problems. PENTRAN has been benchmarked based on the VENUS-3 critical facility, the Kobayashi benchmark problems, and C7G5 MOX eigenvalue problem. The paper presents the results obtained, and discusses the lessons learned.

1. INTRODUCTION

This paper reviews our efforts in benchmarking the PENTRAN (Parallel Environment Neutral-particle TRANsport) 3-D, Sn parallel code [1, 2] using the OECD-NEA benchmark problems. PENTRAN has been used for solving several real-world problems for different applications; however, in this paper, we will focus on the use of NEA benchmarks to evaluate different features of the PENTRAN code. We will present the results of the VENUS-3 benchmark facility [3], the Kobayashi 3-D void duct benchmark problems [4], and the C5G7 MOX criticality problem [5]. Besides evaluating the accuracy of the results, we will discuss the code performance, specifically in a parallel environment, as well as the impact of its unique features, and any limitations we have observed in solving these problems.

.

This paper is organized as follows. In Section II, we briefly discuss the important features of PENTRAN. In Section III, we present important features of each problem, and examine PENTRAN's solution accuracy and parallel performance, and discuss the lessons learned. Section IV concludes this paper.

2. PENTRAN'S UNIQUE FEATURES AND ITS SUPPORTING CODES

PENTRAN is a 3-D Cartesian Sn code developed for distributed-memory and parallel computing environments, written in FORTRAN 90 employing the MPI (message passing interface) library [6]. It has been implemented on numerous different platforms including PCs and workstations, including IBM and SUN, as well as on parallel computers including the IBM SP2/SP3/BG, Cray-SGI, SUN multi-processors and clusters, and more recently on Linux-based PC Clusters. The important features and algorithms of PENTRAN are: memory partitioning, parallel I/O, full phase space domain decomposition, an adaptive differencing strategy, the DTW (directional theta-weighted) [7], and EDW/EDI (exponential directional weighted/exponential directional iterative) [8, 9] differencing schemes, and variable meshing with TPMC (Taylor projection mesh

coupling) [10], different angular quadrature sets with ordinate splitting (OS) [11] and new acceleration schemes [12]. Besides the necessity of solving a problem in a short time, it is important to be able to easily develop/modify a model and process the results in short time -. This is especially true when dealing with complex 3-D problems. For pre-processing, we have developed PENMSHXP. PENMSHXP is a 3-D Cartesian mesh generator that, in addition to the material mesh distribution, allows projection of a source distribution onto the material mesh distribution, and prepares an input file for PENTRAN. For post-processing parallel distributed memory datafiles, PENDATA and PENPRL codes were developed. PENDATA, based on a set of user-defined parameters, prepares tables of flux (moments and angular), material, or source values from outputs files generated in a parallel environment. PENPRL utilizes PENDATA and PENMSHXP outputs, and a 3-D linear interpolation scheme to obtain flux values at arbitrary positions within the model.

Recently, we have developed a burnup module for 3-D burnup calculation [13] and a version of the code for medical physics application (PENTRAN-MP) [14].

3. USE OF THE OECD-NEA BENCHMARK PROBLEMS FOR ANALYSIS OF THE PENTRAN CODE

3.1 Simulation of theVENUS-3 experimental facility

The VENUS critical facility is a zero power reactor located at SCK•CEN, the Belgian Nuclear Research Laboratory. This facility has been used to study LWR core designs and benchmarking of computer codes. In 1988, the VENUS-3 experiment [15] was designed to examine the effect of partial length assemblies on fluence values in the PWR pressure vessel. Because of presence of the partial length assemblies and the resultant three-dimensionality of the core, VENUS-3 has also been used for benchmarking of three-dimensional transport theory codes.

Using PENMSHXP, a 3-D discrete model was developed. [3] The model mesh distribution (Fig. I) represents a quadrant of VENUS-3 with a radial size of 65.573 cm x 65.573 cm and an axial size of 70 cm.

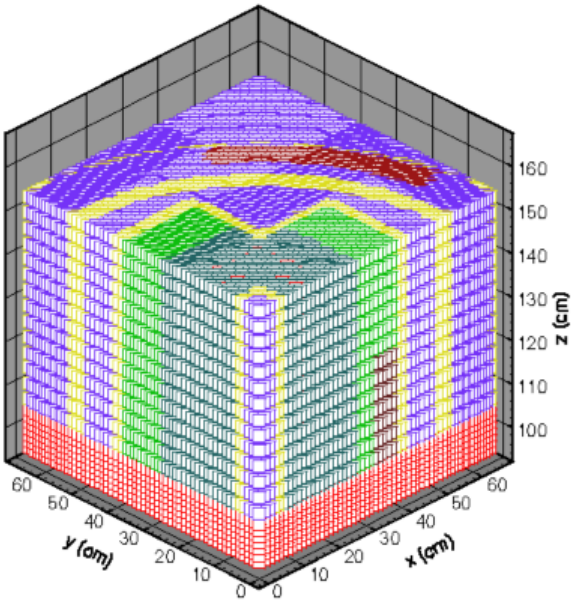

Figure I. PENTRAN model for the VENUS-3 benchmark facility (note that top reflector is not represented in this diagram)

Radially, we have modeled the facility up to the inner wall of the air-filled jacket. Axially, we represented the active height of 50 cm and the upper and lower reflectors, each with a height of 10 cm. This model includes 7x7x4 coarse meshes and 84,784 fine meshes. Twenty-six-group, P3 cross sections were prepared for eight material mixtures using the BUGLE-96 library [16]. This library includes 47 neutron

groups and 20 gamma groups. The eight mixtures are: i) water; ii) inner and outer baffles; iii) 4.0% enriched fuel rods, iv) 3.3% enriched fuel rods, v) the stainless steel region of the partial length assemblies, vi) neutron pad, vii) bottom and top reflectors, and viii) Pyrex rods.

For an S8 level-symmetric quadrature, we have computed 26-group flux distributions on 32 processors of the DoD ASC IBM SP2 by partitioning the model into 8 angular and 4 spatial domain sub-domains. This calculation required only 1.4 hrs wall-clock time.

As a sample in Fig. II, we show the flux distribution for the first group. The white region represents the fuel region that has the highest flux. Presence of partial length assemblies has resulted in a lower flux value in the lower half of core beyond x=~31.6 cm where these assemblies are placed.

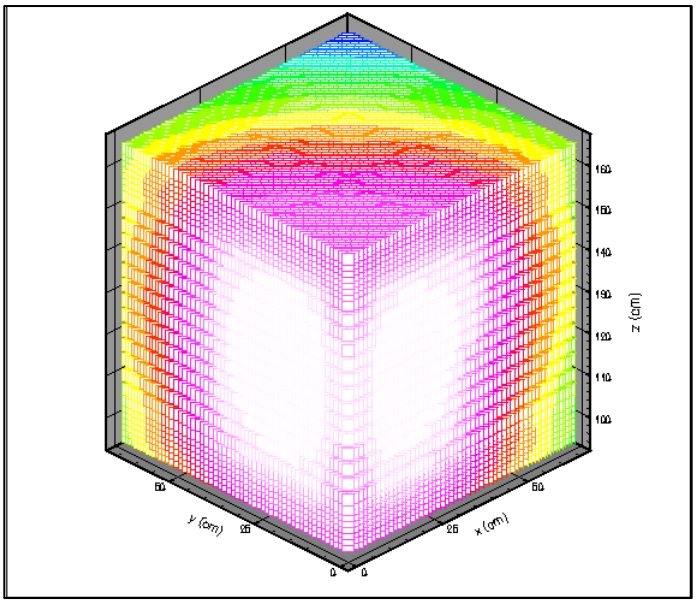

Figure II. Flux distribution for energy group 1

To compare our results to the experimental data, we have calculated normalized reaction rates for 58Ni(n,p), 115In(n,n'), and 27Al(n,α) interactions as

$$r_{ij} = \frac{\sum_{g=1}^{26} \sigma_g^j \phi_g^i}{\sum_{g=1}^{26} \sigma_g^j \chi_g} \qquad (1)$$

where σ_g^j refers to reaction (or response) cross-section isotope j for energy group g, ϕ_g^i refers to flux at position *i* for energy group *g*, and χ_g refers to the fission spectrum for energy group g. Fig. III shows the calculated-to-experimental (C/E) ratios of the normalized reaction rates for the three dosimeters. Overall, PENTRAN calculated results are in excellent agreement with the experimental dosimeter results.

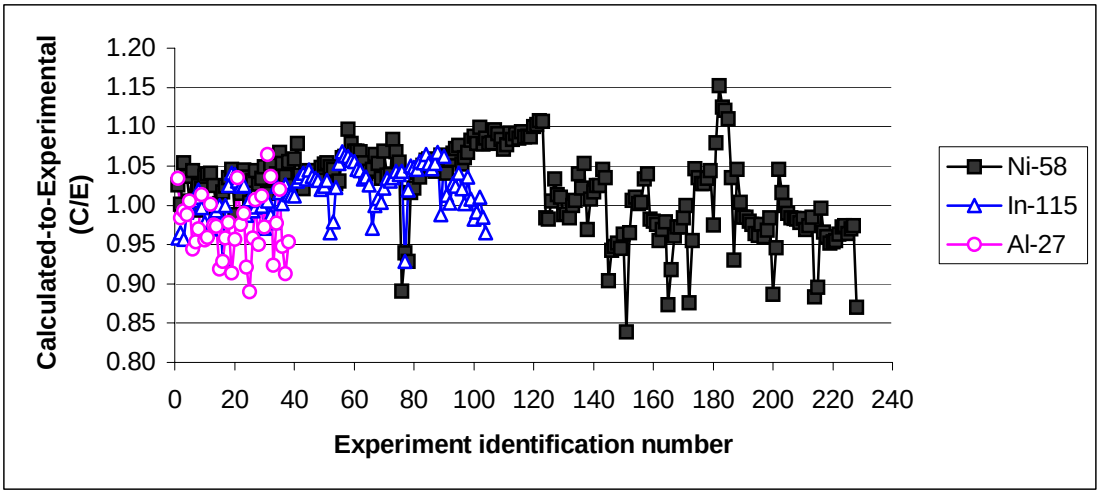

Figure III. Calculated to experimental (C/E) results for different interactions

For the nickel dosimeters, there are 228 C/E values that varied between 0.84 and 1.15; of these, 144 values are within ±5%, 69 are within ±5% to ±10%, and only 15 values are within ±10% to ±15%. For the indium dosimeters, there are 104 C/E values that vary between ~0.93 and ~1.07; of these, 86 values are within ±5%. For the aluminum dosimeters, there are 38 C/E's that vary between ~0.89 and ~1.07; of these, 28 values are within ±5%.

Several timing tests were performed solving the VENUS-3 problem (with 84748 meshes, 80 directions, and 26 groups) using different numbers of processors of an IBM SP2 parallel machine with different space-angle domain decomposition algorithms. The SP2 machines were "wide" SP2 nodes with at least 512 MB of memory per processors. Table I gives the cases considered, along with wall-clock time, speedup, and efficiency (defined as speedup per number of processors). It is important to note that these runs were performed in a BATCH mode (i.e., non-dedicated mode), so some loss of speedup/efficiency is expected, but difficult to assess.

Table I. PENTRAN parallel performance on an IBM SP2 for different number of processors and domain decomposition algorithms

Case	Number of processors	Decomposition algorithm (A/G/S)[1]	Wall-clock time (min)[2]	Speedup	Efficiency (%)
1	4	4/1/1	551.8	1.00	-
2	8	8/1/1	311.9	1.77	88
3	16	8/1/2	153.3	3.60	90
4	32	8/1/4	84.3	6.54	82

[1](A/G/S) refers to the number of angular, group, and spatial sub-domains.
[2]Time is obtained in a BATCH mode.

Case 1 uses only the angular domain decomposition algorithm with four processors that is considered as the base case. Cases 2 through 4 are eight angular sub-domains with different

numbers of spatial sub-domains (1, 2 and 4) on 8, 16, and 32 processors, respectively. Relative to Case 1, Cases 2 to 4 show efficiencies in a range of 82-90%. As expected, the shortest time is achieved for the 32-processor case, although this case yielded the lowest efficiency among the cases tested. Two major factors contribute to this loss of efficiency: i) loss of granularity (or computational load); ii) increase in the message passing overhead. From these results, it is clear that for this problem, angular- spatial domain decomposition in PENTRAN is quite effective for rendering a solution in a minimum amount of wall-clock time.

This benchmark provided two major findings: i) PENTRAN can yield accurate results for deep penetration problems; ii) PENTRAN shows a high parallel scalability and efficiency.

3.2 Kobayashi 3-D Benchmarks

Kobayashi proposed [17] three 3-D problems for examining the accuracy of 3-D transport codes. These problems are defined as parallelepipeds and contain three regions: source, void, and shield. Problems are solved for two situations: i) the material in the source and shield regions is a pure absorber; ii) the material in the source and shield regions were set to a 50% scattering ratio. The total cross-section of this material is 0.1 cm^{-1}, while the total cross-section of the voids is 10^{-4} cm^{-1}.

We tested PENTRAN's numerical capability to solve the Kobayashi 3-D simple benchmarks. [18] The standard discrete ordinates method, with its limited number of directions, generally yields erroneous results that may differ significantly from the true solutions. This is especially true for deep penetration in a purely absorbing or low scattering shield, or at the interface of void and shield. Since the benchmarks have a simple one-group cross-section and P_0 anisotropy, we used the serial version of PENTRAN on a single processor.

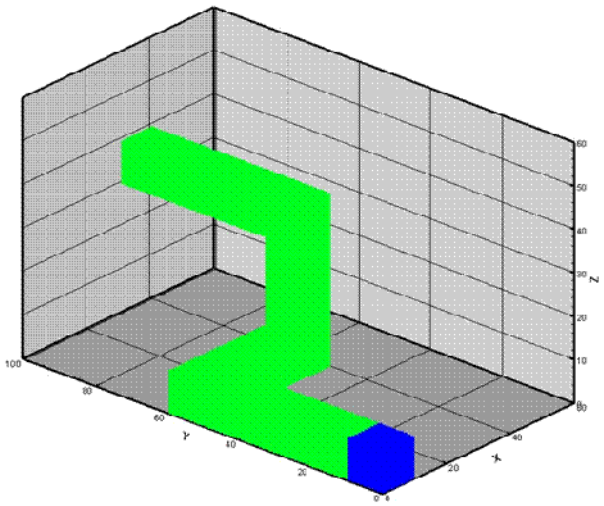

Figure IV. Kobayashi benchmark problem 3

For brevity, we only discuss problem 3, referred to as the shield with a “dog-leg void” duct, shown in Fig. IV. This problem is composed of three regions: source, void duct, and shield. The problem size is 60x100x60 cm^3, and the source region is 10x10x10 cm^3, and the void duct penetrates through model.

PENTRAN results are compared to the analytical and Monte Carlo solutions for three sets of positions. The first set (case 3A) includes positions along the y-axis at every 10 cm between 5 and 95 cm, at x = 5 cm and z = 5cm. The second set (case 3B) includes positions along x-axis at every 10 cm between 5 and 55 cm, at z = 5 cm and y =55 cm. The third set (case 3C) includes positions along x-axis at every 10 cm between 5 and 55 cm, at y = 95 cm and z =35 cm.

For the purely absorbing case, as shown in Fig. V, the PENTRAN model has four *z*-levels of thickness 10 cm each, which in turn are partitioned into 5 axial meshes. The *x*-*y* plane is partitioned into 6x7 coarse meshes. These meshes are refined further into a total of 12581 meshes. Note that the mesh refinement is done mainly along the diagonals between the source and positions of comparison.

Figs. VI.a to VI.c compare the PENTRAN and analytical fluxes for the cases 3A to 3C positions. Along the *y*-axis, case 3A, the two solutions differ by < 6%. Along the x-axis, case 3B, a maximum difference of <~9% occurs at x = 55 cm. Along the *x*-axis, case 3C, a maximum difference of <26% occurs at x =15 cm.

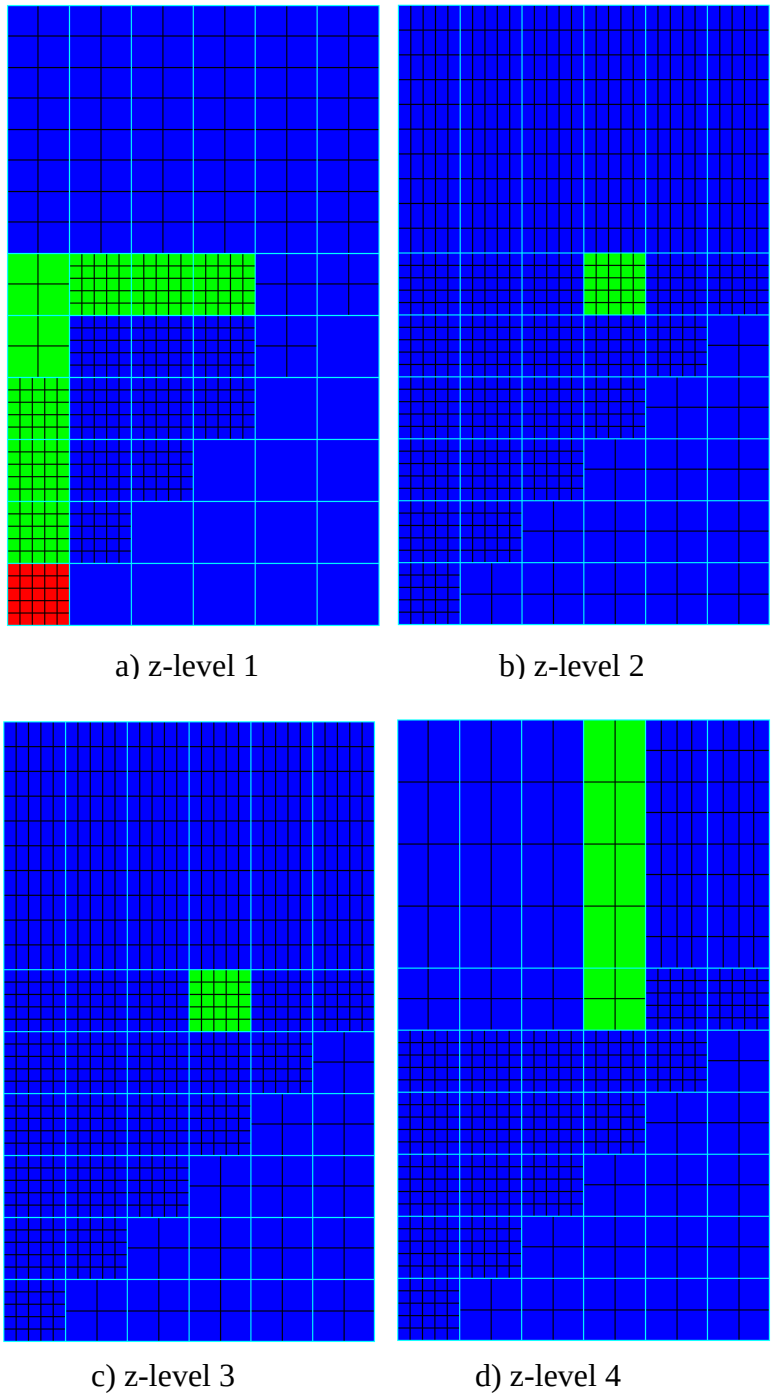

a) z-level 1 b) z-level 2

c) z-level 3 d) z-level 4

Figure V. Schematic of PENTRAN mesh distribution

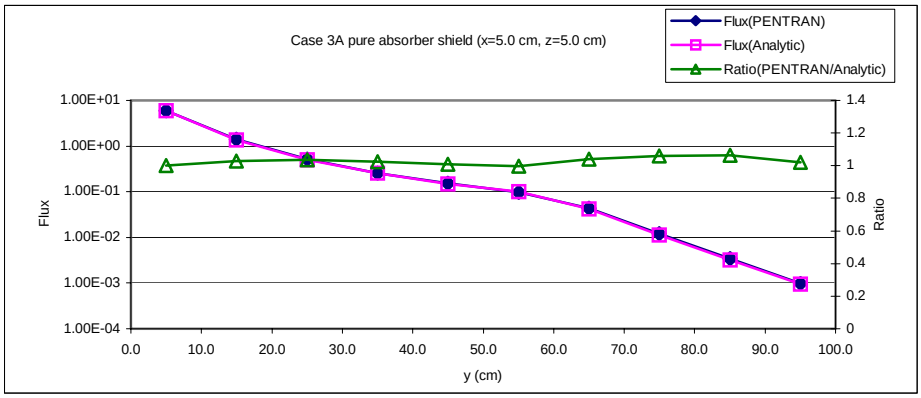

a) Case 3A.

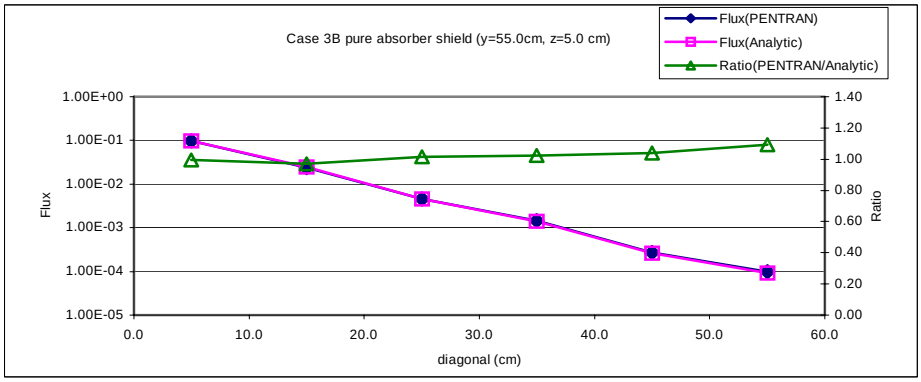

b) Case 3B

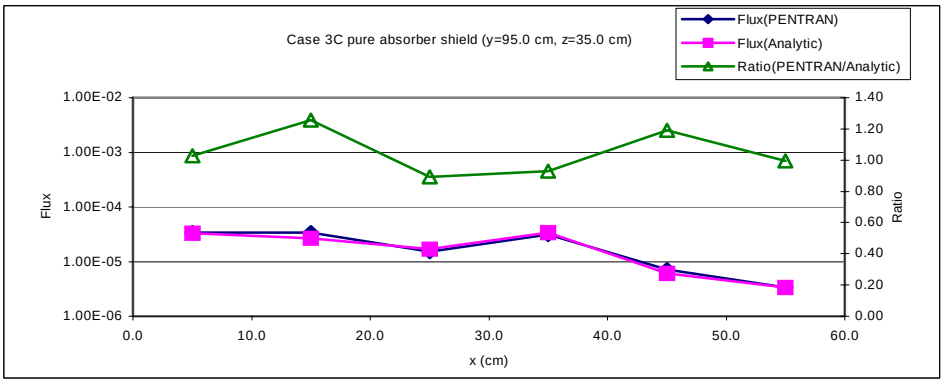

c) Case 3C

Figure VI. Comparison of PENTRAN and analytical solutions for Problem 3

3.2.1 Analysis of PENTRAN Unique Numerical Techniques

Further, we examined [18] the impact of unique numerical techniques of PENTRAN including the adaptive differencing strategy and the Taylor Projection Mesh Coupling (TPMC) formulation.

We examined various cases with different combinations of adaptive differencing algorithms with and without use of the TPMC formulation.

Our analysis revealed that the use of DTW is suitable for the void region, while EDW is useful for the absorbing region. Further, it was demonstrated that TPMC is instrumental in achieving an accurate solution. These results confirm that TPMC is needed where neighbor cells have significantly different grid densities and/or material properties.

Through solving this benchmark problem, we learned the effectiveness of the TPMC numerical treatment for discontinuous mesh cases in conjunction with the adaptive differencing strategy that resulted in relatively excellent agreement between a purely Sn algorithm and analytic solution for a difficult problem.

Recently, we utilized this benchmark problem to examine a newly developed hybrid Sn and Characteristic algorithm [19]. Using the hybrid algorithm, S_N solver treats the source region, characteristics solver treats the void &absorber regions. Here, a uniform mesh of 1x1x1 cm^3 and the P_N-T_N angular quadrature of order S30 are used. [20]

Our results indicate differences of <11%, <9%, and <27% for cases 3A, 3B, and 3C, respectively. It is important to mention that was achieved for a uniform mesh with the hybrid algorithm. For example, Fig. VII shows, ratio of the hybrid solution to the analytical results at the end face of the dog-leg problem at y=35 cm, z=95 cm for different x values.

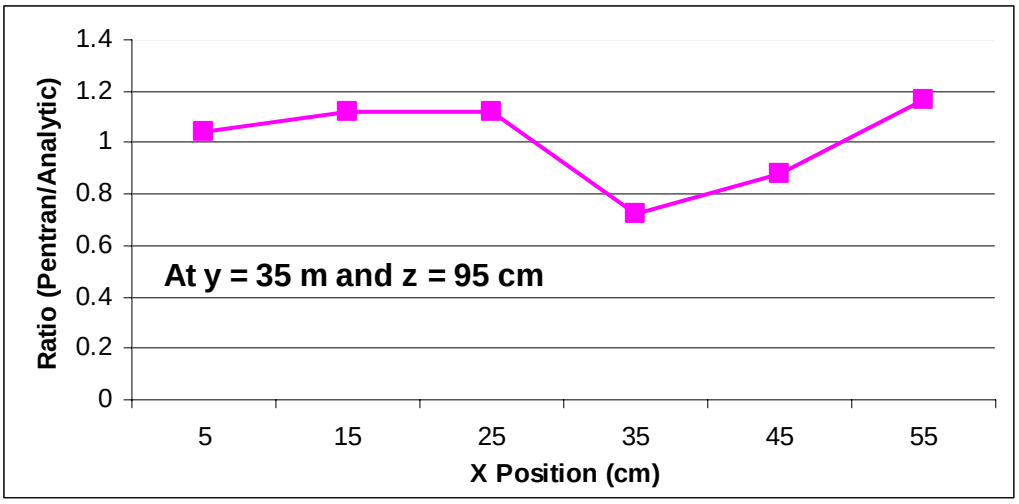

Figure VII. Comparison of the hybrid algorithm to analytical problem for Kobayashi problem 3 at 3C position

3.3 C5G7 MOX Criticality Benchmark

The seven-group form of the C5 MOX fuel assembly problem (C5G7MOX) was proposed for testing the ability of current transport codes for solving the effective multiplication factor (K_{eff}) and power distribution in a fuel assembly without spatial homogenization. [21]

Fig. VIII shows radial and axial projections of the C5G7 benchmark problem. As shown, the

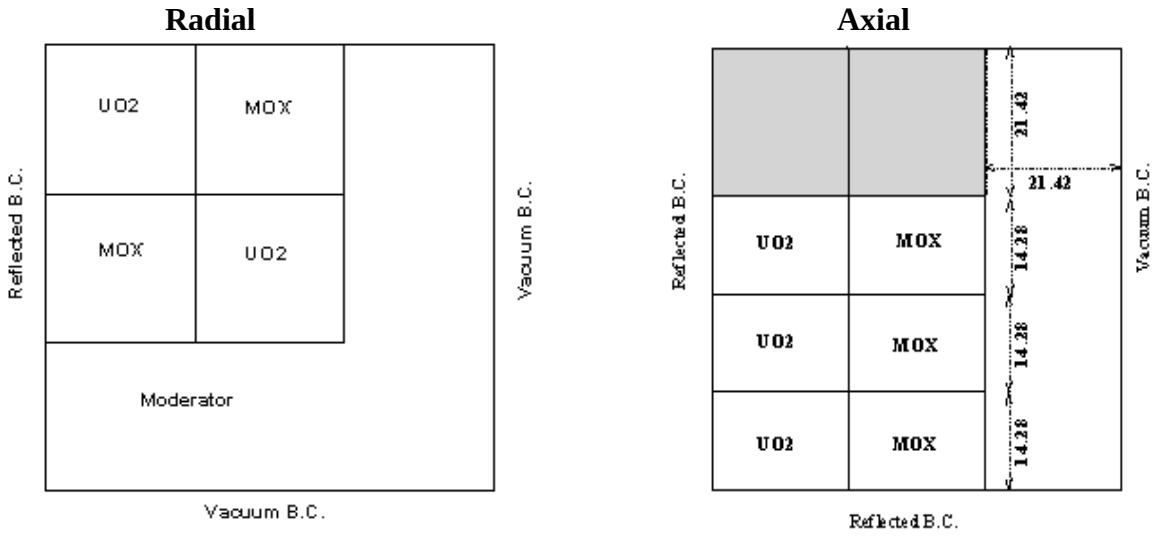

Figure VIII. Schematic of the C5G7 benchmark problem (unrodded)

problem includes two UO2 and two MOC assemblies, and the gray region identify the presence of control rods which are out of the core. This case is referred to as the unrodded case, and two other cases were devices as rodded-A and rodded-B, which are shown in Figs. IX.a and IX.b, respectively.

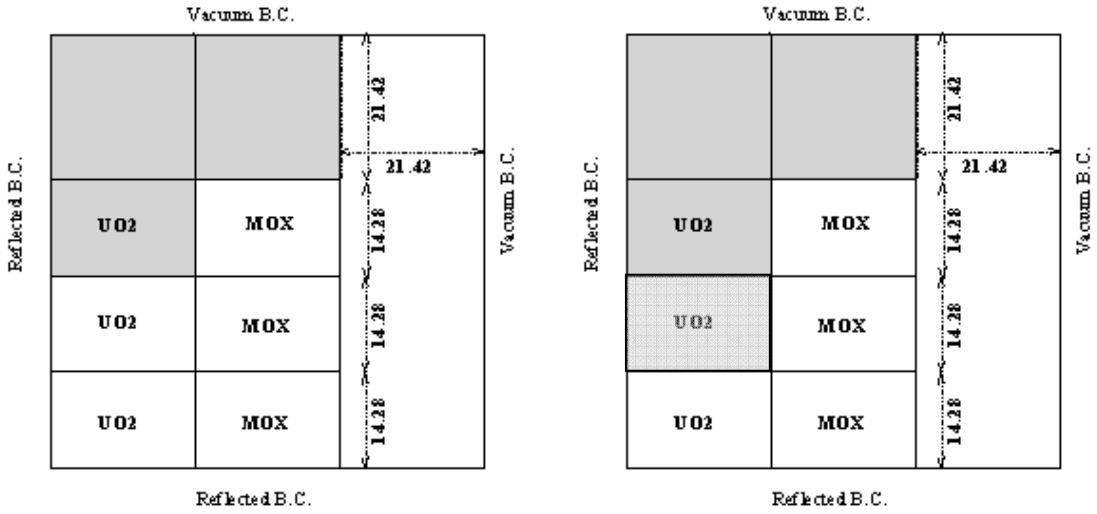

a) Rodded-A Rodded-B

Figure IX. Schematics of the Rodded cases

We utilized a new version of the PENTRAN code referred as PENTRAN-SSn (Parallel Environment Neutral-Particle TRANsport - preconditioned with Simplified even-parity Sn).[22]. PENTRAN-SSn uses PENSSn (A parallel 3-D simplified even-parity Sn code) as pre-conditioner [23]. For all cases, we used ~950,000, S6 quadrature set, DTW differencing formulation, with 8 spatial decompositions and 2 angular decomposition processed on 16 processors.

Table II gives the results of eigenvalues for the three cases, their differences to the reference Monte Carlo solutions, and corresponding wall-clock times.

Table II. Comparison of eigenvalues and corresponding wall-clock times for difference cases

Case	Reference	PENTRAN-SSn	$\frac{\Delta k}{k}$ (PCM)	Wall-clock time (hr)
Unrodded	1.143080 ± 0.0026	1.144770	147.8	15.24
Rodded-A	1.128060 ± 0.0027	1.128900	74.5	15.94
Rodded-B	1.077770 ± 0.0028	1.07350	390.6	17.66

Despite of the good agreement in the eigenvaluses, the results of pin-power distributions show a maxim difference of ~8%. Fig. X shows the percent relative pin-power difference distribution for the Rodded-A case. We attributed this result to the use of a relatively low quadrature order of S_6 and relatively coarse axial mesh intervals of 7-8 cm, which were dictated by the limitations in the available memory.

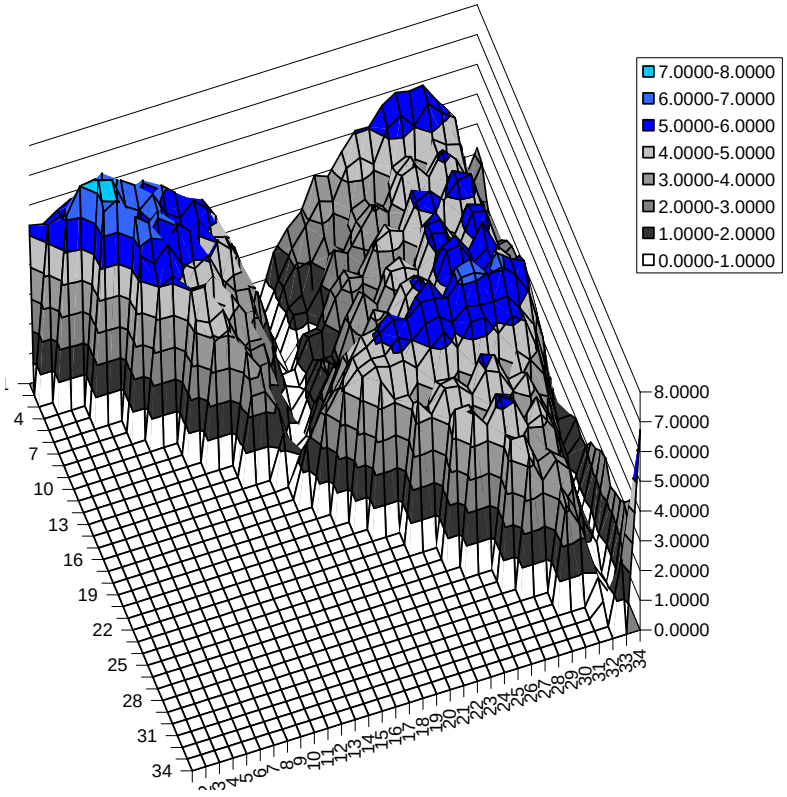

Figure X. Percent relative pin-power difference for Rodded-A case

This benchmark indicates that PENTRAN-SSn can solve assembly-wise eigenvalue problems without homogenization in a reasonable amount of time. However, it was demonstrated that the use of PEN-SSn algorithm as a pre-conditioner is essential, because otherwise the wall-clock time increases by a factor of 6 which is not practical. This benchmark also indicated the effectiveness of the new PEN-SSn algorithm as a pre-conditioner for Sn eignevalue calculations.

4. CONCLUSIONS

This paper reviewed our efforts in benchmarking of the PENTRAN code using three OECD/NEA benchmarking problems. These benchmarks have been enormously valuable for our efforts in verification, testing and improvement of various aspects of the PENTRAN code.

Development, coordination, and participation of international communities in these benchmarks would not have been possible without unusual dedication of Dr. Enrico Sartori. We thank him for his contributions and friendship and wish all the best in his retirement!

REFERENCES

1. Sjoden, G. E., "PENTRAN- A Parallel 3-D Sn Transport Code with Complete Phase Space Decomposition, Adaptive Differencing, and Iterative Solution Methods", *PhD Dissertation*, The Pennsylvania State University (1997).
2. Sjoden, G. E. and A. Haghighat, "PENTRAN- Parallel Environment Neutral- particle TRANsport in 3-D Cartesian Geometry," P*roc. Joint Int. Conf. on Mathematical Models and Supercomputing for Nucl. Applications*, Saratoga Springs, New York, (1997)
3. Haghighat, A., H. A. Abderrahim, and G.E. Sjoden, "Accuracy and Parallel Performance of PENTRAN Using the VENUS-3 Benchmark Experiment", Reactor Dosimetry, *ASTM STP* 1398, John G. Williams, et al., Eds., ASTM, West Conshohocken, PA, 2000.
4. Kucukboyaci, V., Haghighat, A., Sjoden, G. E., and Petrovic B., "Modeling of BWR for Neutron and Gamma Fields Using PENTRAN™," Reactor Dosimetry, *ASTM STP 1398*, John G. Williams, David W. Vehar, Frank H. Ruddy, and David M. Gilliam, Eds., American Society for Testing and Materials, West Conshohocken, PA, 2000.
5. Haghighat, A., G. E. Sjoden and V. Kucukboyaci, "Effectiveness of PENTRAN's Unique Numerics for Simulation of the Kobayashi Benchmarks," *Progress in Nuclear Energy Journal*, 2001.
6. Gropp W., Lusk E., and Skjellum A., *USING MPI- Portable Parallel Programming with Message Passing Interface*, MIT Press, 1995.
7. Petrovic, B. and A. Haghighat, "New Directional Theta-Weighted SN Differencing Scheme and Reduction of Estimated Pressure Vessel Fluence Uncertainty," *Reactor Dosimetry*, edited by H. A. Abderrahim, P. D'hondt, and B. Osmera, World Scientific Publishing Co. (1998).
8. Sjoden, G. E. and A. Haghighat, "The Exponential Directional Weighted (EDW) Sn Differencing Scheme in 3-D Cartesian Geometry," *Proceedings of the 1997 Joint International Conference on Mathematical Methods and Supercomputing for Nuclear Applications*, Vol. 2, 1267, Saratoga Springs, NY (1997).
9. Sjoden, G. E., "An Efficient Exponential Directional Iterative Differencing Scheme for 3-D Sn Computations in XYZ Geometry," *Nuclear Science and Engineering*, Vol 155, pp. 179-189 (2007).
10. Sjoden, G. E. and A. Haghighat, "Taylor Projection Mesh Coupling Between 3-D Discontinuous Grids for Sn," *Trans. Am. Nucl. Soc.*, 74, 178-179 (1996).

11. Longoni, G. and A. Haghighat, "Development and Application of the Regional Angular Refinement Technique and its Application to Non-Conventional Problems", *Proceedings of PHYSOR 2002*, Seoul, Korea, October 2002
12. Kucukboyaci, V. and A. Haghighat, "Angular Multigrid Acceleration for Parallel SN Method with Application to Shielding Problems," *Proceedings of the PHYSOR 2000*, Pittsburgh, PA, May 7-11, 2000.
13. Manalo, K.., T. Plower, M. Rowe, T. Mock, and G. Sjoden, "PENBURN – A 3-D Zone-Based Depletion/Burnup Solver," *Proceedings of PHYSOR2008*, Interlaken, Switzerland, September 2008.
14. Al-Basheer, A., G. Sjoden, and M. Ghita, "Electron Dose Kernels to Account for Secondary Particle Transport in Deterministic Simulations", *Nuclear Technology Journal*, September, 2008, 19 pages.
15. Leenders, L., LWR-PVS Benchmark Experiment VENUS-3 (with Partial Length Shielded Assemblies), SCK•CEN, Mol, Belgium, *FCP/VEN/01* (Sept. 1988).
16. White, J. E. et al., BUGLE-96: A revised multigroup cross section library for LWR applications based on ENDF/B-VI release 3, in *American Nuclear Society Radiation Protection & Shielding Topical Meeting*, Falmouth, MA, USA, 1996, Oak Ridge National Laboratory.
17. Kobayashi, K., "A Proposal for 3-D Radiation Transport Benchmarks for Simple Geometries with Void Region," *Proceedings of the 3-D Deterministic Radiation Transport Computer Programs – Features, Applications and Perspectives*, OECD/NEA, Dec. 2-3, 1996.
18. Haghighat, A., G.E. Sjoden, and V.N. Kucukboyaci, "Effectiveness of PENTRAN's Unique Numerics for Simulation of the Kobayashi Benchmarks," a special issue of the *Progress in Nuclear Energy*, Vol. 39, No. 2, pp. 191-206, 2001.
19. Yi, C., and A. Haghighat, "A Hybrid Block-Oriented Discrete Ordinates and Characteristics Method Algorithm for Solving Linear Boltzmann Equation," *Joint International Topical Meeting on Mathematics & Computation and Supercomputing in Nuclear Applications (M&C + SNA 2007)* Monterey, California, April 15-19, 2007, on CD-ROM, American Nuclear Society, LaGrange Park, IL 2007.
20. Yi, C., Hybrid Discrete Ordinates and Characteristic Method for Solving the Linear Boltzmann Equation, *PhD Dissertation*, University of Florida, 2007.
21. Benchmark on Deterministic Transport Calculations Without Spatial Homogenization – MOX Fuel Assembly 3-D Extension Case, *NEA/NSC/DOC(2005)16*, 2005.
22. Longoni, G, "Advanced Quadrature Sets and Acceleration and Preconditioning Techniques for the Discrete Ordinates Method in Parallel Computing Environments," *PhD Dissertation*, University of Florida, December 2004.
23. Longoni, G. and A. Haghighat, "The Even-Parity Simplified SN Equations Applied to a MOX Fuel Assembly Benchmark Problem on Distributed Memory Environments," *PHYSOR 2004 -The Physics of Fuel Cycles and Advanced Nuclear Systems: Global Developments*, Chicago, Illinois, April 25-29, 2004, on CD-ROM, American Nuclear Society, Lagrange Park, IL. (2004).